Journal of General Virology (2007), **88**, 1634–1642 DOI 10.1099/vir.0.82729-0

Cymbidium ringspot virus defective interfering RNA replication in yeast cells occurs on endoplasmic reticulum-derived membranes in the absence of peroxisomes

Luisa Rubino, Beatriz Navarro and Marcello Russo

Istituto di Virologia Vegetale del CNR, Sezione di Bari, c/o Dipartimento di Protezione delle Piante e Microbiologia Applicata, Università degli Studi, Bari, Italy

Correspondence
Luisa Rubino
l.rubino@ba.ivv.cnr.it

Received 21 November 2006
Accepted 7 January 2007

The replication of *Cymbidium* ringspot virus (CymRSV) defective interfering (DI) RNA in cells of the yeast *Saccharomyces cerevisiae* normally takes place in association with the peroxisomal membrane, thus paralleling the replication events in infected plant cells. However, previous results with a peroxisome-deficient mutant strain of yeast had suggested that the presence of peroxisomes is not a strict requirement for CymRSV DI RNA replication. Thus, a novel approach was used to study the putative alternative sites of replication by using *S. cerevisiae* strain YPH499 which does not contain normal peroxisomes. In this strain, CymRSV p33 and p92 accumulated over portions of the nuclear membrane and on membranous overgrowths which were identified as endoplasmic reticulum (ER) strands, following immunofluorescence and immunoelectron microscope observations. The proteins were not released by high-pH treatment, but were susceptible to proteolytic digestion, thus indicating peripheral and not integrated association. ER-associated p33 and p92 proteins supported *in trans* the replication of DI RNA. The capacity of plus-strand RNA viruses to replicate in association with different types of cell membranes was thus confirmed.

INTRODUCTION

The replication complex of virtually all positive-strand animal and plant RNA viruses is known to associate with host cell membranes, which are normally rearranged to form partially closed vesicular enclaves. It is believed that the major advantage for viral genome replication in such a confined environment is to protect it from host defence reactions. The nature of the cell membrane recruited for the assembly of the virus replication complex varies, depending on the virus. In fact, vesicles can derive from the endoplasmic reticulum (ER) (picornaviruses, potyviruses, comoviruses, nepoviruses and bromoviruses) or from the limiting membrane of organelles such as lysosomes or endosomes (alphaviruses), vacuoles (cucumoviruses), mitochondria (nodaviruses, some tombusviruses, carmoviruses, ampeloviruses and maculaviruses), peroxisomes (several tombusviruses) and chloroplasts (tymoviruses and some marafiviruses) (reviewed by Salonen *et al.*, 2005; Villanueva *et al.*, 2005; Martelli & Boudon-Padieu, 2006).

The initial assembly step of the replication complex requires targeting of the viral replicase to the specific cell membrane where it anchors. Targeting and anchoring depend on signals in the viral proteins which allow specific association with organelle membranes. Following this, membranes undergo drastic morphological changes resulting in the production of a number of flask-shaped vesicles.

The association of viral replicase proteins with the limiting membrane of peroxisomes and mitochondria has been studied in detail with members of the genus *Tombusvirus* (family *Tombusviridae*). The genome of these viruses consists of a single RNA molecule of approximately 4800 nt containing five open reading frames (ORFs) (Russo *et al.*, 1994; White & Nagy, 2004). The two 5′-proximal ORFs code for two proteins required for the replication of genomic RNA and other small molecules such as satellite and defective interfering (DI) RNAs. These replicase proteins have a size ranging from 33 (p33) to 36 (p36) kDa and 92 (p92) to 95 (p95) kDa, depending on the viral species, and are translated directly from genomic RNA. Internal ORFs code for the capsid (ORF 3), movement (ORFs 4 and 5) and gene silencing suppressor (ORF 5) proteins, respectively, and are expressed via the synthesis of two subgenomic RNAs. The tombusviruses *Cymbidium ringspot virus* (CymRSV) and *Carnation Italian ringspot virus* (CIRV) have been widely used for the analysis of targeting signals of the replicase, taking advantage of the diversity of the intracellular localization of their replication complex. In fact, replication of CymRSV takes place in vesicles derived from the peroxisomal membrane (Russo *et al.*, 1983, 1987),

Additional figures are available as supplementary material in JGV Online.

whereas CIRV replicates in vesicles derived from the outer membrane of mitochondria (Di Franco *et al.*, 1984; Russo *et al.*, 1987). By exchanging genome fragments between infectious cDNA clones of the two viruses, it was shown that the signals dictating the site of replication were present in the protein encoded by ORF 1 (i.e. p33 or p36, for CymRSV and CIRV, respectively) (Burgyan *et al.*, 1996). These signals consisted of short stretches of hydrophilic amino acids plus two hydrophobic transmembrane domains (Weber-Lotfi *et al.*, 2002; Navarro *et al.*, 2004). Peroxisomes also proved to be involved in the assembly of the CymRSV replication complex in yeast cells (Navarro *et al.*, 2006). However, when a yeast strain genetically deficient for peroxisome biogenesis was used, the replicase proteins (p33 and p92) and DI RNA were targeted to the ER, which became the site of DI RNA replication (Navarro *et al.*, 2006).

In the present work, the association of the CymRSV DI RNA replication complex with ER membranes was further analysed.

METHODS

Yeast strains and growth conditions. Yeast strains used were YPH499 (*MAT***a**, *ura3*-52 *lys2*-801 *ade2*-101 *trp1*-Δ63 *his3*-Δ200 *leu2*-Δ1) (Sikorski & Hieter, 1989) and UTL-7A (*MAT***a** *leu2-3,112 ura3-52 trp1*) (Erdmann *et al.*, 1989). UTL-7A transformants were previously described and grown accordingly (Navarro *et al.*, 2006). YPH499 cells were transformed using the lithium acetate–polyethylene glycol method (Ito *et al.*, 1983) and grown as described previously (Pantaleo *et al.*, 2003).

Plasmids. pALDsRedAKL and pKat84 express constitutively (ADH1 promoter) the red fluorescent protein DsRed containing the peroxisomal matrix targeting signal AKL (Wang *et al.*, 2001; Navarro *et al.*, 2004), and the Pex27p peroxisomal membrane protein fused to the green fluorescent protein (GFP) (Rottensteiner *et al.*, 2003), respectively. CymRSV p33 and p92 proteins were expressed constitutively with vectors pA and YE (Pantaleo *et al.*, 2003; Navarro *et al.*, 2006), respectively. These proteins were tagged at their N termini with Myc and haemagglutinin (HA) epitopes, respectively; in addition, p92 was mutated to carry a tyrosine codon in place of the p33 stop codon (Navarro *et al.*, 2006). Alternatively, both p33 and p92 were expressed using only one plasmid (YE) by readthrough of the p33 stop codon from the p92 wild-type (wt) coding sequence (p92wt) (Navarro *et al.*, 2006). DI-3 RNA (Burgyan *et al.*, 1992) was cloned in the vector pBMI3S under the control of the galactose-inducible GAL1 promoter (Ishikawa *et al.*, 1997; Pantaleo *et al.*, 2003). GFP and fusion protein p33–GFP were expressed using the galactose-inducible vector pYES2 (Invitrogen) (Navarro *et al.*, 2004).

For the intracellular detection of DI RNA progeny, the *Bam*HI–*Bgl*II fragment, encoding six MS2 recognition hairpins, was excised from plasmid pSL-MS2-6 (Bertrand *et al.*, 1998) and cloned between blocks II and III of DI-3 RNA (Burgyan *et al.*, 1992), where a *Bam*HI site had been introduced by site-directed mutagenesis (QuikChange kit; Stratagene) to give clone DI-3/MS2. The GFP-tagged MS2 coat protein containing a nuclear localization signal (NLS) was expressed with plasmid pG14-MS2-GFP (Bertrand *et al.*, 1998).

Miscellaneous techniques. Immunofluorescence, electron microscopy and immunoelectron microscopy methods were detailed in previous papers (Navarro *et al.*, 2004, 2006). For simultaneous detection of p33 and p92, ultrathin sections of LR White-embedded cells were treated with mouse anti-Myc (p33 tag) and rabbit anti-HA (p92 tag) antibodies and then with goat anti-mouse and anti-rabbit antibodies labelled with 10 and 15 nm gold particles, respectively. RNA was extracted as described by Schmitt *et al.* (1990) and analysed by Northern blotting as described by Navarro *et al.* (2006). Protein extraction and Western blot analysis were as previously described (Pantaleo *et al.*, 2003; Navarro *et al.*, 2004). Carbonate treatment was as described by Rubino & Russo (1998); proteinase K digestion and analysis of digests using a discontinuous Tris-Tricine system electrophoresis (Schagger & von Jagow, 1987) were as described by Weber-Lotfi *et al.* (2002).

RESULTS

Localization of CymRSV p33 in strain YPH499

S. cerevisiae strains YPH499 and YPH500 (two mating types with otherwise identical genotype) have been used for studying the replication of Brome mosaic virus (BMV) (YPH500; Janda & Ahlquist, 1993), Flock House virus (FHV) (YPH500; Price *et al.*, 1996) and CIRV (YPH499; Pantaleo *et al.*, 2003). Previous investigations on CymRSV replicase-driven DI RNA replication (Navarro *et al.*, 2006) used UTL-7A, a strain in which peroxisomes are induced and increase in size and number in medium containing oleate as sole carbon source (Erdmann *et al.*, 1989). By contrast, strain YPH499 does not grow on an oleate medium, which suggests that its cells do not contain mature peroxisomes (Cavero *et al.*, 2003).

To verify this point YPH499 cells were transformed with plasmids pALDsRedAKL, expressing a red-fluorescing protein with a peroxisomal matrix targeting signal (Wang *et al.*, 2001), or pKat84, expressing the peroxisomal membrane protein Pex27p fused to GFP (Rottensteiner *et al.*, 2003). UTL-7A cells transformed with the same plasmids were used as control (Navarro *et al.*, 2004). Fluorescence microscope observations showed that DsRedAKL was not targeted to any organelle of YPH499 cells, for it was diffused in the cytosol, whereas Pex27p–GFP localized to scattered spots, often just one, in some cells, probably representing a peroxisome (Fig. 1, upper row). In UTL-7A cells, as expected, both DsRedAKL and Pex27p–GFP highlighted numerous spots, identified as peroxisomes (Fig. 1, lower row). Shifting to oleate medium increased only slightly the growth of YPH499 cells and did not alter the peroxisomal content, in contrast with UTL-7A cells whose peroxisomes enlarge and proliferate in this medium (Götte *et al.*, 1998; Navarro *et al.*, 2004) (see Supplementary Fig. S1, available in JGV Online).

In conclusion, these results suggest that small peroxisomes may also be present in YPH499 cells grown on glucose which, however, do not enlarge and proliferate following shifting to a growth medium containing oleic acid as sole carbon source. The lack of responsiveness to oleate is likely due to defects in the matrix import machinery, as shown by the inefficiency of the matrix targeting signal in the DsRedAKL protein.

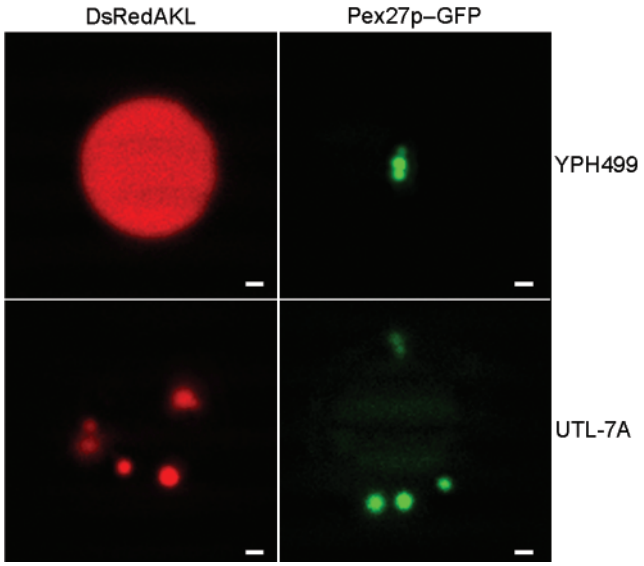

Fig. 1. Identification of peroxisomes in *S. cerevisiae* cells of strain YPH499 (upper row) and UTL-7a (lower row) grown in a glucose-containing medium by expression of proteins targeted to the matrix (DsRedAKL) or to the membrane (Pex27p–GFP). Bars, 1 μm.

It was previously shown that in UTL-7A cells, expression of p33 fused to GFP was localized to peroxisomal aggregates and induced membrane proliferation (Navarro *et al.*, 2004). A similar experiment was done in YPH499 cells, by expressing the fusion protein p33–GFP with vector pYES2 in the absence of other viral products. Cells growing in the presence of galactose showed accumulation of GFP in large bodies around the nucleus and in patches scattered in the cytoplasm, which reacted with antibodies to the ER marker protein Kar2p (Fig. 2a, upper row), but not to the Golgi apparatus (Emp47p) (Fig. 2a, middle row) or mitochondrial (Tom40p) (Fig. 2a, lower row) markers. Control cells expressing unfused GFP showed the expected pattern of green fluorescence diffused in the cytoplasm (see Supplementary Fig. S2a, available in JGV Online). Co-expression of p33 and Pex27p–GFP showed that the large accumulation of p33 was not accompanied by peroxisome proliferation (Fig. 2b). In conclusion, CymRSV p33 seems to be associated with ER membranes in YPH499 cells and does not alter the peroxisomal pattern.

The intracellular localization of both replicase proteins p33 and p92 was investigated using Myc-tagged and HA-tagged versions of these proteins, respectively. The distribution of p33 was reanalysed by double immunofluorescence microscopy using anti-Myc mouse antibodies in conjunction with rabbit antibodies to Kar2p, Emp47p and Tom40p markers of ER, Golgi apparatus and mitochondria, respectively. It was confirmed that p33 modified the structure of the ER (Fig. 3a), as compared to control cells (see Supplementary Fig. S2b), and was not associated with mitochondria or Golgi (see Supplementary Fig. S3a, b).

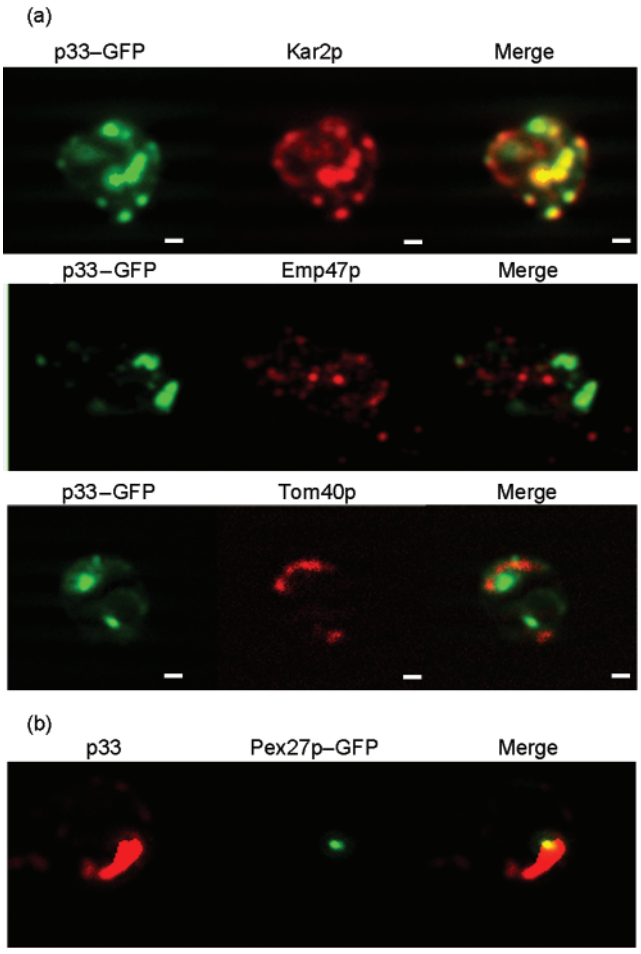

Fig. 2. (a) Association of GFP-tagged p33 with the ER. Yeast cells YPH499 expressing p33–GFP fusion protein were immunostained using rabbit primary antibodies to the protein markers of ER (Kar2p, upper row), Golgi (Emp47p, middle row) and mitochondria (Tom40p, lower row) and rhodamine red-conjugated goat anti-rabbit secondary antibodies. Selected images of each label and their superimposition (Merge) are shown. (b) Expression of p33 does not modify the peroxisomal pattern of YPH499 cells. p33 was immunostained with anti-Myc antibodies and peroxisomes were visualized by the localization of the membrane-targeted protein Pex27p fused to GFP. Bars, 1 μm.

When mouse anti-Myc antibodies were used in conjunction with rabbit anti-HA antibodies, it was shown that the p92 accumulation largely coincided with p33 (Fig. 3b). Results on the distribution of p33 also suggest that p92 accumulates on the perinuclear and cortical ER. No alteration of the peroxisome pattern was induced by coexpression of p33 and p92 (see Supplementary Fig. S3c).

Electron microscopy of YPH499 yeast cells

Ultrathin sections of YPH499 cells transformed with empty vectors (Fig. 4a) showed the presence of the nucleus, short ER strands, mitochondria and vacuoles. Golgi cisternae,

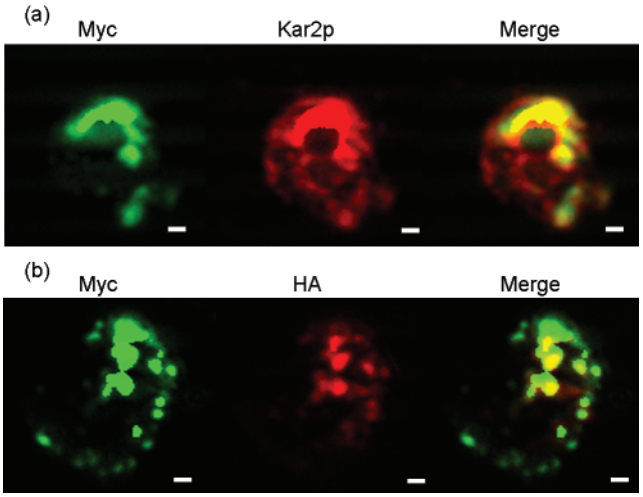

Fig. 3. Colocalization of p33 and p92. Yeasts were cotransformed with plasmids expressing Myc-tagged p33 and HA-tagged p92. (a) Cells were double-labelled using mouse anti-Myc and rabbit anti-Kar2p followed by goat anti-mouse antibodies conjugated to Alexa Fluor 488 and anti-rabbit antibodies conjugated to rhodamine. (b) Cells were double-labelled using mouse anti-Myc and rabbit anti-HA followed by goat anti-mouse antibodies conjugated to Alexa Fluor 488 and anti-rabbit antibodies conjugated to rhodamine. Selected images of each label and their superimposition (Merge) are shown. Bars, 1 μm.

which are not organized in stacks in *S. cerevisiae* (Rossanese *et al.*, 1999), are not morphologically distinguishable in these cells. Cells expressing p33 and p92 alone or together with DI RNA (see below) showed cytoplasmic accumulations of membranes either scattered in the cytoplasm or appressed in stacks to the nuclear membrane (Fig. 4b–f). Altogether, these membrane accumulations recall the ER-derived structures identified in fluorescence microscopy as sites of accumulation of p33 and p92 and, when present, of DI RNA (see below).

To confirm the association of viral replicase proteins with membranous overgrowths, yeast cells were transformed as above, fixed with aldehydes and embedded in LR White. Ten nanometre gold particles, detecting p33, were consistently found on isolated or stacked ER strands (Fig. 5b–f) and were absent in other parts of the cell or in control cells transformed with empty vectors (Fig. 5a). The accumulation of p92, as visualized by 15 nm gold particles, was much lower than for p33, in line with the immunofluorescence results. The localization of the two proteins on ER membranous strands coincided.

p33–ER membrane affinity

To investigate the degree of affinity of p33 and p92 with ER membranes, proteins were extracted from transformed cells, fractionated by differential centrifugation and analysed by Western blotting using anti-Myc and anti-HA antibodies.

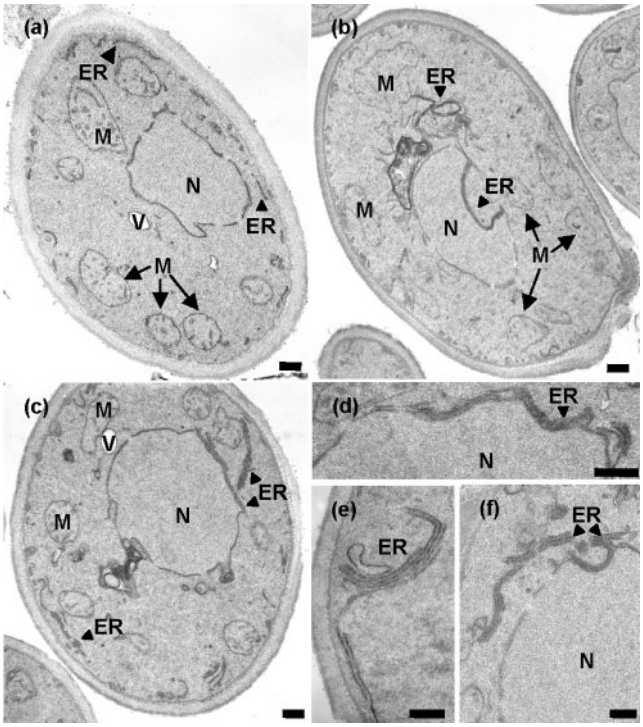

Fig. 4. Electron micrographs of yeast cells expressing p33 and p92 alone (b, f) or both together with DI RNA (c–e) or no viral product (a). Cells were fixed with aldehydes, post-fixed with sodium permanganate and embedded in Spurr resin. Cells expressing the viral replicase proteins showed proliferation of ER. N, Nucleus; M, mitochondria; V, vacuole. Bars, 250 nm.

Both proteins were recovered in the pellet obtained by centrifuging the cell lysate at 30 000 ***g*** (P30) and were virtually absent in the supernatant (Fig. 6a). This result could indicate association of the viral proteins with cell membranes.

To discriminate between a true integration in the membrane or a peripheral association due to protein–protein or protein–lipid interactions, the P30 fraction was exposed to high pH in sodium carbonate (Na_2CO_3) buffer and further centrifuged. As shown in Fig. 6(b), both p33 and p92 were mostly recovered in the pellet after this treatment. This finding would be consistent with the presence of two hydrophobic membrane-spanning domains which were previously shown to promote the integration in the peroxisomal membrane of plant and yeast cells, leaving most of the sequence upstream and downstream the integrated segment exposed in the cytoplasm (Rubino & Russo, 1998; Navarro *et al.*, 2004).

If the same type of integration of p33 into the ER membrane occurred, only the parts of the protein exposed in the cytoplasm would be accessible for a protease treatment in the absence of detergent. To verify this point, the membrane pellet fraction from transformed YPH499 cells expressing p33 and p92 was digested with proteinase K in

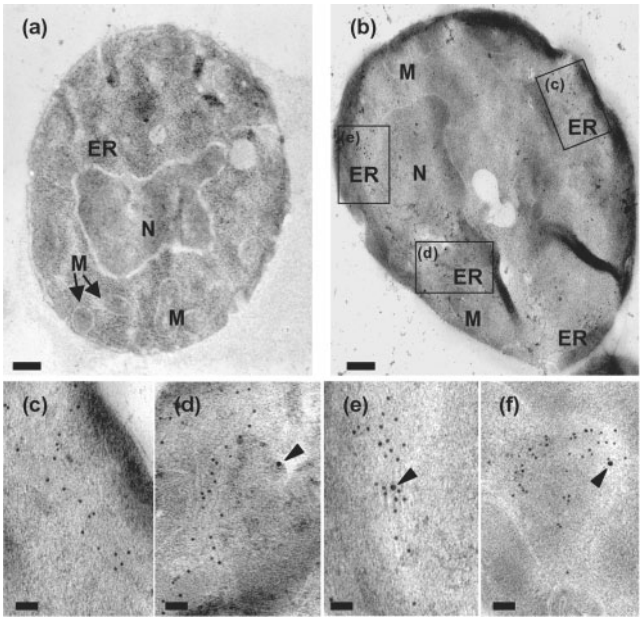

Fig. 5. Electron micrographs of yeast cells expressing p33 and p92 together with DI RNA (b–f) or no viral product (a). Cells were fixed with aldehydes and embedded in LR White resin for gold immunolabelling. As compared with control cells (a), cells expressing viral products contain membranous overgrowths with which p33 and p92 associate (10 and 15 nm gold particles, respectively). (c–e) Close-ups of regions boxed in (b). Arrowheads point to 15 nm gold particles. Bars, 250 nm (a, b); 100 nm (c–f).

the presence or absence of Triton X-100. As control, similar protein extracts from transformant yeast strain UTL-7A cells, which were previously shown to contain a membrane-embedded protease-resistant fragment of p33 (Navarro *et al.*, 2004), were used. As shown in Fig. 6(c) (left panel), no protease-resistant fragment was detected by anti-p33 antiserum in the YPH499 cell extracts with or without detergent treatment. Conversely, UTL-7A extracts contained two small resistant fragments of approximately 14 and 12 kDa, which were no longer detected if the membranes were treated with Triton X-100 (Fig. 6c, right panel). Altogether these results indicate that p33 and p92 (i) were present in the P30 fraction because they are associated with membranes; (ii) are peripheral but not membrane-integral proteins; (iii) are associated with the cytoplasmic side of the ER.

DI RNA replication and localization of the replication complex in YPH499 cells

To see whether p33 and p92 targeted to ER membranes in YPH499 yeast cells were competent to form a replication complex capable of replicating *in trans* DI RNA molecules, cells were cotransformed to express the tagged versions of the replicase proteins (Myc–p33 and HA–p92) under the control of constitutive promoter ADH1, and to express DI RNA under the control of the galactose-inducible GAL1 promoter (Navarro *et al.*, 2006). Northern blot analysis of RNA extracts from transformed YPH499 cells showed that robust DI RNA replication took place only in the presence of both replicase proteins p33 and p92 (Fig. 7a). These proteins were expressed either by two separate plasmids (lane 4) or by only one plasmid expressing wt p92 (lane 3), whereas no progeny RNA was detected when p92 (lane 1) or p33 (lane 2) were omitted. As in previous experiments (Pantaleo *et al.*, 2004; Rubino *et al.*, 2004; Navarro *et al.*, 2006), the progeny DI RNA was composed of monomers and dimers (Fig. 7a, lanes 3 and 4).

To localize the site of accumulation of DI RNA progeny, a novel technique was used based on the MS2 phage (Bertrand *et al.*, 1998) which had been successfully applied to study tombusvirus replication in yeast cells by Panavas *et al.* (2005). Briefly, six copies of the MS2 phage coat protein (CP) recognition hairpins were cloned between blocks II and III of DI RNA in both positive and negative orientation. Yeast cells were transformed to coexpress mutant DI-3 RNA (DI-3/MS2), the MS2 CP fused to GFP containing NLS and the CymRSV p92wt. Only cells expressing both p33 and p92 would be able to replicate DI-3/MS2, switching the localization of GFP from the nucleus to the site of DI RNA replication. Transformed yeasts were grown as described previously (Pantaleo *et al.*, 2003; Rubino *et al.*, 2004) and divided in two aliquots, from one of which RNA was extracted and the other was fixed for immunofluorescence analysis. Northern blot analysis of RNA extracts showed that mutant DI RNA molecules containing the MS2 recognition sequence in both positive (Fig. 7b, lane 1) or negative (Fig. 7b, lane 3) orientations were replication competent, but at a level much lower than the wt (Fig. 7b, lane 4). As expected, no DI RNA replication occurred in the absence of CymRSV replicase proteins (Fig. 7b, lane 2). In the immunofluorescence analysis, a small number of cells showed negative-strand DI RNA localized mainly over the nuclear membrane, whereas positive-strand DI RNA progeny partially colocalized with the ER marker Kar2p (Fig. 7c), indicating the ER as the site of DI RNA replication.

Mutational analysis of putative ER targeting signals

Two putative ER targeting signals are present near the N terminus of CymRSV p33, consisting of dibasic motifs, namely lysine (K)–arginine (R) at positions 5 and 6 (K_5R_6) and KK at positions 11 and 12 ($K_{11}K_{12}$) (McCartney *et al.*, 2005). To evaluate the role of these regions in the ER targeting of p33 and assembly of active replication complex, each pair was substituted with glycine (G) residues (mutants G_5G_6 and $G_{11}G_{12}$, respectively). Yeasts were transformed to express these p33 mutants alone or together with p92 and DI RNA and analysed for the ability to replicate DI RNA. Northern blot analysis of RNA extracts from these transformants did not reveal a significant reduction in the amount of replicated DI RNA (see Supplementary Fig. S4, available in JGV Online).

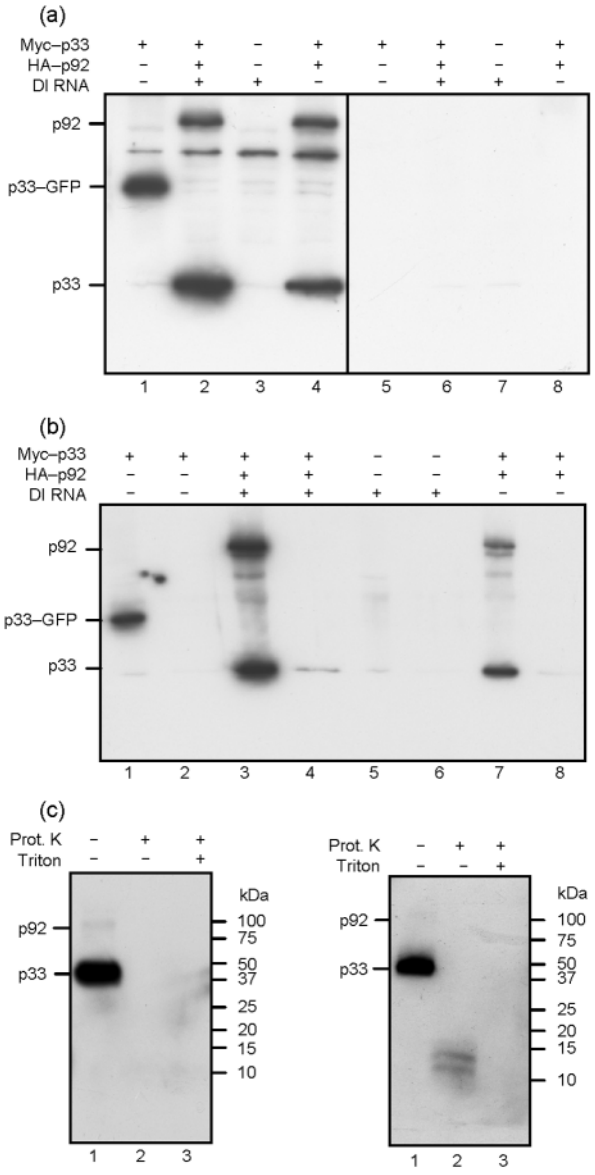

Fig. 6. Western blot analysis of the intracellular distribution of p33–GFP, p33 and p92. (a) Protein extracts from yeast cells expressing p33–GFP (lanes 1 and 5); p33, p92 and DI RNA (lanes 2 and 6); DI RNA alone (lanes 3 and 7) or p33 and p92 alone (lanes 4 and 8) were centrifuged to yield P30 pellet (lanes 1–4) and supernatant (lanes 5–8) fractions. Viral proteins accumulated with the pellet fraction. (b) P30 pellet fractions from yeast cells expressing p33–GFP (lanes 1 and 2); p33, p92 and DI RNA (lanes 3 and 4); DI RNA alone (lanes 5 and 6) or p33 and p92 alone (lanes 7 and 8) were extracted in 0.1 M Na_2CO_3 and further centrifuged to yield pellet (lanes 1, 3, 5 and 7) and supernatant (lanes 2, 4, 6 and 8) fractions. The proteins were not removed from membranes after the carbonate treatment. (c) Protein extracts from YPH499 (left panel) and UTL-7A (right panel) cells expressing p33, p92 and DI RNA were treated with proteinase K in the presence (lane 3) or absence (lane 2) of Triton X-100. Lane 1 contains untreated sample. No protected fragment was detected in YPH499 cell protein extracts. Western blot analysis was performed using anti-Myc and anti-HA antibodies (a and b) and anti-p33 antibodies (c). Positions of p92, p33–GFP and p33 are indicated on the left. In (c) the positions of molecular size markers (kDa) are indicated on the right.

Immunofluorescence analysis of mutant G_5G_6-expressing cells showed that p33 colocalized with portions of perinuclear ER (Fig. 8a) which, however, did not show the conspicuous enlargement as in cells expressing wt p33 (Fig. 3a), resulting from the apposition to the nucleus of proliferated membranes (compare Fig. 8c with Fig. 4b–f). In addition, large spots present in the cytoplasm reacted with anti-Myc but not anti-Kar2p antibodies (Fig. 8a). Conversely, accumulation of p33 mutant $G_{11}G_{12}$ was more similar to wt p33, because of the presence of large perinuclear bodies and smaller cytoplasmic accumulations reacting with anti-Myc and Kar2p antibodies (Fig. 8b). In fact, corresponding electron microscope analysis showed limited membrane proliferation apposed to the nucleus (Fig. 8d). The cytoplasmic electron-dense bodies (triangles in Fig. 8c, d) likely represent aggregates of p33 corresponding to the green-fluorescent spots of Fig. 8 (a, b).

DISCUSSION

In this study the *S. cerevisiae* strain YPH499 was used to investigate how the CymRSV replication complex could be constructed in the virtual absence of peroxisomes, since the membrane of these organelles is the site of replication of genomic and DI RNA in plant and yeast cells (Russo *et al.*, 1983, 1987; Navarro *et al.*, 2006). The working hypothesis was that replication could be retargeted to an alternative membrane system, as in other cases where such retargeting was experimentally obtained by modifying the structure of the viral replicase proteins (Miller *et al.*, 2003) or by altering the ratio of the components constituting the active viral replicase (Schwartz *et al.*, 2004).

For CymRSV, replication retargeting was investigated in a host where biogenesis of peroxisomes is impaired. In this respect, preliminary experiments with yeast strain UTL-7A*pex19*Δ suggested the capability of the CymRSV replication complex to localize to the ER instead of peroxisomes, which are absent in these cells (Götte *et al.*, 1998; Navarro *et al.*, 2006). In the present study strain YPH499 was used, whose cells are unable to form mature peroxisomes. Nevertheless, DI RNA replication based on the CymRSV replicase was still very efficient because the replicase proteins p33 and p92 were targeted to and associated with alternative membranes such as the ER. However, the affinity of CymRSV replicase for ER membranes was not consistent with integration, rather indicating a peripheral association. In fact, no protease-resistant fragment was detected, suggesting that the protein is completely exposed to the cytoplasm with no luminal protrusion. Incidentally, the detection of two fragments in UTL-7A extracts, which contrasts with the detection of only one fragment of smaller size in previous studies (Navarro *et al.*, 2004),

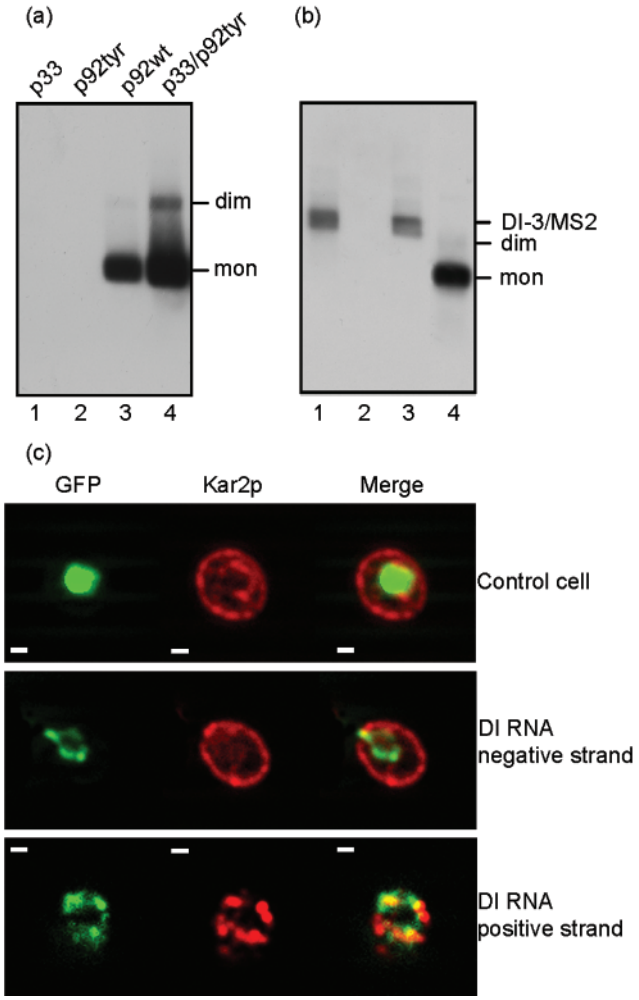

Fig. 7. DI RNA replication in YPH499 cells. (a) Northern blot analysis of RNA extracted from cells expressing DI RNA together with either p33 (lane 1) or p92 (p92tyr, lane 2) alone or both proteins from one (p92wt, lane 3) or two (p33/p92tyr, lane 4) plasmids. Replication occurs only in the presence of both proteins. The position of monomeric (mon) and dimeric (dim) DI RNA molecules is indicated. (b) Northern blot analysis of RNA extracted from cells expressing p92wt and DI RNA containing six MS2-binding sites in positive (lane 1) or negative (lane 3) orientation relative to the DI RNA sequence. Lanes 2 and 4 contain extracts from cells expressing wt DI RNA alone or with p92wt, respectively. Replication of DI RNA/MS2 took place, although reduced compared to wt DI RNA. The position of progeny DI RNA/MS2, monomeric (mon) and dimeric (dim) wt DI RNA molecules is indicated. (c) Intracellular localization of progeny DI RNA. The upper row shows one cell expressing the MS2 CP fused to GFP containing a nuclear localization signal and immunostained for the ER marker Kar2p: GFP is localized exclusively in the nucleus. Cells in the middle and lower rows show the localization of DI RNA negative and positive strands, respectively, overlapping in part the nuclear membrane and ER. Bars, 1 μm.

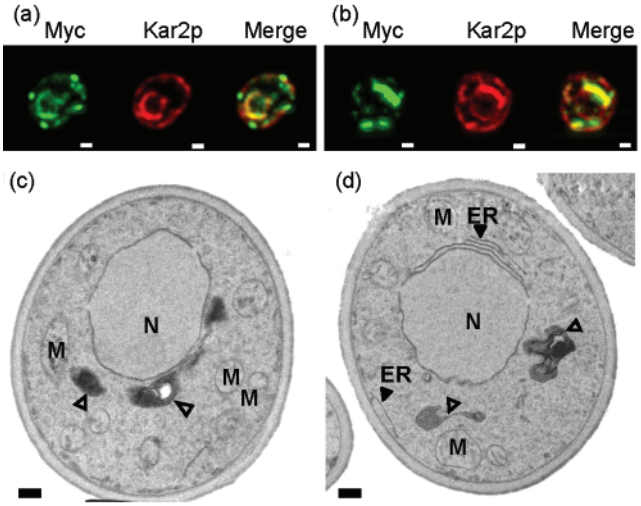

Fig. 8. Intracellular distribution of p33 mutants G_5G_6 (a and c) and $G_{11}G_{12}$ (b and d). (a, b) Cells expressing DI RNA, p92 and p33 mutants G_5G_6 (a) and $G_{11}G_{12}$ (b) immunostained with anti-Myc and anti-Kar2p antibodies. p33 mutant G_5G_6 accumulates on the nuclear membrane and in cytoplasmic aggregates; p33 mutant $G_{11}G_{12}$ accumulates on enlarged portions of the nuclear membrane, the ER and in small cytoplasmic aggregates. (c, d) Electron micrographs of cells transformed with p33 mutants G_5G_6 (c) and $G_{11}G_{12}$ (d) showing the occurrence of dark bodies (open triangles) in the cytoplasm which may represent p33 accumulation. Cells transformed with p33 mutant $G_{11}G_{12}$ (d) resemble cells expressing wt p33 (Fig. 4b–f) because of the occurrence of ER strands appressed to the nuclear envelope. ER, Endoplasmic reticulum; N, nucleus; M, mitochondria. Bars, 1 μm (a, b); 250 nm (c, d).

is likely due to the better resolution in the Tris–Tricine electrophoresis system (Schagger & von Jagow, 1987). The peripheral association of CymRSV with ER membranes recalls that of BMV protein 1a with the same membranes (den Boon *et al.*, 2001), but whereas in the latter case the finding is consistent with the absence of hydrophobic sequences capable of spanning the membrane, this is not the case of CymRSV p33 (and p92) which contains two such sequences participating in the formation of a peroxisomal targeting signal (Rubino & Russo, 1998; Navarro *et al.*, 2004). Thus, targeting and association of CymRSV p33 with the ER probably do not involve the two transmembrane domains.

Other studies have demonstrated that determinants of ER membrane association of viral proteins include amphipathic helices and transmembrane hydrophobic sequences for animal viruses such as poliovirus (van Kuppeveld *et al.*, 1996; Paul *et al.*, 1994), hepatitis C virus (Brass *et al.*, 2002) and a plant virus (tomato ringspot virus; Zhang *et al.*, 2005). The involvement of hydrophobic amphipathic helices and/or transmembrane segments was also predicted on the basis of sequence similarities for other viruses, i.e.

cowpea mosaic virus (Carette *et al.*, 2002), BMV (den Boon *et al.*, 2001) and tobacco mosaic virus (dos Reis Figueira *et al.*, 2002).

Using a prediction method for monotopic proteins inserted and anchored parallel to the membrane (in-plane membrane anchors, IPM; Sapay *et al.*, 2006), no such sequence segments were found in CymRSV p33. Further computer analysis of CymRSV p33, performed using the SOPM computer program for secondary structure prediction (Combet *et al.*, 2000) and the ANTHEPROT program (Deleage *et al.*, 2001) for prediction and projection of the putative amphipathic helices, showed the occurrence of an amphipathic helix between residues 52 and 64, which may be involved in the peripheral interactions of p33 with the ER membranes.

In plant cells infected by several tombusviruses, p33 is targeted to the peroxisomal membrane, where it interacts with p92, viral RNA and perhaps host factors to form an active replication complex as shown experimentally for tomato bushy stunt virus (TBSV) (Panaviene *et al.*, 2004; Rajendran & Nagy, 2004) and elicits the formation of the characteristic flask-shaped vesicles constituting the multivesicular bodies (MVB) (Martelli *et al.*, 1988). The involvement of ER in the formation of MVB was suggested by Russo *et al.* (1983) and demonstrated by McCartney *et al.* (2005). The latter authors demonstrated the occurrence of an indirect ER targeting signal operating in a peroxisome-to-ER pathway, followed by retrieval of ER membranes to peroxisomes. We suggest that the pair of positively charged residues (K_5R_6) in the N-terminal region identified by McCartney *et al.* (2005) is also likely to contribute to the formation of an ER targeting signal in yeast cells in the absence of peroxisomes, indicating that the preliminary localization of p33 to the peroxisomal membrane is not a necessary step for targeting to ER. Rather, the ER membranes could be the initial target for CymRSV replicase proteins prior to trafficking to peroxisomes, in the absence of which the ER-to-peroxisome pathway would be blocked. However, this event does not affect virus replication since the ER membranes were shown to be fully competent for the assembly of the virus replication complex, in alternative to the peroxisomal membrane.

Finally, it is worth noting the adaptability of plus-strand RNA viruses to use diverse types of membranes if alterations are forced in the structure of their replicase (Burgyan *et al.*, 1996; Miller *et al.*, 2003; Schwartz *et al.*, 2004) or when the organelle content of the host cell is modified (this paper). Furthermore, we show that replicase proteins launched by non-replicating mRNAs, which cannot themselves evolve or adapt at the amino acid level, have enough plasticity to adjust without any change in their structural properties. Consequently, in wt virus infections, where mRNA and protein evolution could occur, adaptation may be even greater. This fact may not support an antiviral strategy based on the manipulation of the structure of a particular membrane by pharmacological or genetic means, as suggested by Lee & Ahlquist (2003).

ACKNOWLEDGEMENTS

We thank Robert H. Singer for pG14-MS2-GFP and pSL-MS2-6 plasmids, A. Antonacci for skilful technical assistance, G. P. Martelli and V. Pantaleo for advice and critical reading of the manuscript and E. Sbisà, Istituto di Tecnologie Biomediche del CNR, Sezione di Bari, Italy, for the use of the fluorescence microscope. This research was partially supported by MIUR, Project Cluster CO3, Legge 488/92, 'Studi di geni di interesse biomedico e alimentare'.

REFERENCES

Bertrand, E., Chartrand, P., Schaefer, M., Shenoy, S. M., Singer, R. H. & Long, R. M. (1998). Localization of ASH1 mRNA particles in living yeast. *Mol Cell* **2**, 437–445.

Brass, V., Bieck, E., Montserret, R., Wolk, B., Hellings, J. A., Blum, H. F., Penin, F. & Moradpour, D. (2002). An amino-terminal amphipathic alpha-helix mediates membrane association of the hepatitis C virus nonstructural protein 5A. *J Biol Chem* **277**, 8130–8139.

Burgyan, J., Dalmay, T., Rubino, L. & Russo, M. (1992). The replication of cymbidium ringspot tombusvirus defective interfering-satellite RNA hybrid molecules. *Virology* **190**, 579–586.

Burgyan, J., Rubino, L. & Russo, M. (1996). The 5′-terminal region of a tombusvirus genome determines the origin of multivesicular bodies. *J Gen Virol* **77**, 1967–1974.

Carette, J. E., van Lent, J., MacFarlane, S. A., Wellink, J. & van Kammen, A. (2002). Cowpea mosaic virus 32- and 60-kilodalton replication proteins target and change the morphology of endoplasmic reticulum membranes. *J Virol* **76**, 6293–6301.

Cavero, S., Vozza, A., del Arco, A., Palmieri, L., Villa, A., Runswick, M. J., Walker, J. E., Cerdan, S., Palmieri, F. & Satrustegui, J. (2003). Identification and metabolic role of the mitochondrial aspartate-glutamate transporter in *Saccharomyces cerevisiae*. *Mol Microbiol* **50**, 1257–1269.

Combet, C., Blanchet, C., Geourjon, C. & Deleage, G. (2000). NPS@: network protein sequence analysis. *Trends Biochem Sci* **25**, 147–150.

Deleage, G., Combet, C., Blanchet, C. & Geourjon, C. (2001). ANTHEPROT: an integrated protein sequence analysis software with client/server capabilities. *Comput Biol Med* **31**, 259–267.

den Boon, J. A., Chen, J. & Ahlquist, P. (2001). Identification of sequences in Brome mosaic virus replication protein 1a that mediate association with endoplasmic reticulum membranes. *J Virol* **75**, 12370–12381.

Di Franco, A., Russo, M. & Martelli, G. P. (1984). Ultrastructure and origin of multivesicular bodies induced by carnation Italian ringspot virus. *J Gen Virol* **65**, 1233–1237.

dos Reis Figueira, A., Golem, S., Goregaoker, S. P. & Culver, J. N. (2002). A nuclear localization signal and a membrane association domain contribute to the cellular localization of the Tobacco mosaic virus 126-kDa replicase protein. *Virology* **301**, 81–89.

Erdmann, R. M., Veenhuis, D., Mertens, D. & Kunau, W. H. (1989). Isolation of peroxisome-deficient mutant of *Saccharomyces cerevisiae*. *Proc Natl Acad Sci U S A* **86**, 5419–5423.

Götte, K., Girzalski, W., Linkert, M., Baumgart, E., Kammerer, S., Kunau, W.-H. & Erdmann, R. (1998). Pex19p, a farnesylated protein essential for peroxisome biogenesis. *Mol Cell Biol* **18**, 616–628.

Ishikawa, M., Janda, M., Krol, M. A. & Ahlquist, P. (1997). In vivo DNA expression of functional Brome mosaic virus RNA replicons in *Saccharomyces cerevisiae*. *J Virol* **71**, 7781–7790.

Ito, H., Fukuda, Y., Murata, K. & Kimura, A. (1983). Transformation of intact yeast cells treated with alkali cations. *J Bacteriol* **153**, 163–168.

Janda, M. & Ahlquist, P. (1993). RNA dependent-replication, transcription, and persistence of brome mosaic virus RNA replicon in *S. cerevisiae*. *Cell* **72**, 961–970.

Lee, W. M. & Ahlquist, P. (2003). Membrane synthesis, specific lipid requirements, and localized lipid composition changes associated with positive-strand RNA virus RNA replication protein. *J Virol* **77**, 12819–12828.

Martelli, G. P. & Boudon-Padieu, E. (Editors) (2006). Directory of infectious diseases of grapevines. In *Options Mediterranéennes* B55.

Martelli, G. P., Gallitelli, D. & Russo, M. (1988). *Tombusviruses*. In *The Plant Viruses*, vol. 1, *Polyhedral Virions with Monopartite RNA Genomes*, pp. 13–72. Edited by R. Koenig. New York: Plenum Press.

McCartney, A. W., Greenwood, J. S., Fabian, M. R., White, K. A. & Mullen, R. T. (2005). Localization of the tomato bushy virus replication protein p33 reveals a novel peroxisome-to-endoplasmic reticulum sorting pathway. *Plant Cell* **17**, 3513–3531.

Miller, D. J., Schwartz, M. D., Dye, B. T. & Ahlquist, P. (2003). Engineered retargeting of viral RNA replication complexes to an alternative intracellular membrane. *J Virol* **77**, 12193–12202.

Navarro, B., Rubino, L. & Russo, M. (2004). Expression of the *Cymbidium ringspot virus* 33-kilodalton protein in *Saccharomyces cerevisiae* and molecular dissection of the peroxisomal targeting signal. *J Virol* **78**, 4744–4752.

Navarro, B., Russo, M., Pantaleo, V. & Rubino, L. (2006). Cytological analysis of *Saccharomyces cerevisiae* cells supporting cymbidium ringspot virus defective interfering RNA replication. *J Gen Virol* **87**, 705–714.

Panavas, T., Hawkins, C. M., Panaviene, Z. & Nagy, P. D. (2005). The role of the p33 : p33/p92 interaction domain in RNA replication and intracellular localization of p33 and p92 proteins of Cucumber necrosis tombusvirus. *Virology* **338**, 81–95.

Panaviene, Z., Panavas, T., Serva, S. & Nagy, P. D. (2004). Purification of the Cucumber necrosis virus replicase from yeast cells: role of coexpressed viral RNA in stimulation of replicase activity. *J Virol* **78**, 8254–8263.

Pantaleo, V., Rubino, L. & Russo, M. (2003). Replication of *Carnation Italian ringspot virus* defective interfering RNA in *Saccharomyces cerevisiae*. *J Virol* **77**, 2116–2123.

Pantaleo, V., Rubino, L. & Russo, M. (2004). The *Carnation Italian ringspot virus* p36 and p95 replicase proteins cooperate in stabilizing defective interfering RNA. *J Gen Virol* **85**, 2429–2433.

Paul, A. V., Molla, A. & Wimmer, E. (1994). Studies of a putative amphipathic helix in the N-terminus of poliovirus protein 2C. *Virology* **199**, 188–199.

Price, B. D., Rueckert, R. R. & Ahlquist, P. (1996). Complete replication of an animal virus and maintenance of expression vectors derived from it in *Saccharomyces cerevisiae*. *Proc Natl Acad Sci U S A* **93**, 9465–9470.

Rajendran, K. S. & Nagy, P. D. (2004). Interaction between the replicase proteins of Tomato bushy stunt virus in vitro and in vivo. *Virology* **326**, 250–261.

Rossanese, O. W., Soderholm, J., Bevis, B. J., Sears, I. B., O'Connor, J., Williamson, E. K. & Glick, B. S. (1999). Golgi structure correlates with transitional endoplasmic reticulum organization in *Pichia pastoris* and *Saccharomyces cerevisiae*. *J Cell Biol* **145**, 69–81.

Rottensteiner, H., Stein, K., Sonnenhol, E. & Erdmann, R. (2003). Conserved function of Pex11p and the novel Pex25p and Pex27p in peroxisome biogenesis. *Mol Biol Cell* **14**, 4316–4328.

Rubino, L. & Russo, M. (1998). Membrane targeting sequences in tombusvirus infections. *Virology* **252**, 431–437.

Rubino, L., Pantaleo, V., Navarro, B. & Russo, M. (2004). Expression of tombusvirus open reading frames 1 and 2 is sufficient for the replication of defective interfering, but not satellite RNA. *J Gen Virol* **85**, 3115–3122.

Russo, M., Di Franco, A. & Martelli, G. P. (1983). The fine structure of *Cymbidium* ringspot virus infections in host tissues. III. Role of peroxisomes in the genesis of multivesicular bodies. *J Ultrastruct Res* **82**, 52–63.

Russo, M., Di Franco, A. & Martelli, G. P. (1987). Cytopathology in the identification and classification of tombusviruses. *Intervirology* **28**, 134–143.

Russo, M., Burgyan, J. & Martelli, G. P. (1994). Molecular biology of *Tombusviridae*. *Adv Virus Res* **44**, 381–428.

Salonen, A., Ahola, T. & Kääriäinen, L. (2005). Viral RNA replication in association with cellular membranes. *Curr Top Microbiol Immunol* **285**, 139–173.

Sapay, N., Guermeur, Y. & Deléage, G. (2006). Prediction of amphipathic in-plane membrane anchors in monotopic proteins using a SVM classifier. *BMC Bioinformatics* **7**, 255.

Schagger, H. & von Jagow, G. (1987). Tricine-sodium dodecyl sulfate-polyacrylamide gel electrophoresis for the separation of proteins in the range from 1 to 100 kDa. *Anal Biochem* **166**, 368–379.

Schmitt, M. E., Brown, T. A. & Trumpower, B. L. (1990). A rapid and simple method for preparation of RNA from *Saccharomyces cerevisiae*. *Nucleic Acids Res* **18**, 3091–3092.

Schwartz, M., Chen, J., Lee, W. M., Janda, M. & Ahlquist, P. (2004). Alternate, virus-induced membrane rearrangements support positive-strand RNA virus genome replication. *Proc Natl Acad Sci U S A* **101**, 11263–11268.

Sikorski, R. S. & Hieter, P. (1989). A system of shuttle vectors and yeast host strains designed for efficient manipulation of DNA in *Saccharomyces cerevisiae*. *Genetics* **122**, 19–27.

van Kuppeveld, F. J., van den Hurk, P. J., Zoll, J., Galama, J. M. & Melchers, W. J. (1996). Mutagenesis of the coxsackie B3 2B/2C cleavage site: determinants of processing efficiency and effects on viral replication. *J Virol* **70**, 7632–7640.

Villanueva, R. A., Rouille, Y. & Dubuisson, J. (2005). Interactions between virus proteins and host cell membranes during the viral life cycle. *Int Rev Cytol* **245**, 171–244.

Wang, X., Unruh, M. J. & Goodman, J. M. (2001). Discrete targeting signals direct Pmp47 to oleate-induced peroxisomes in *Saccharomyces cerevisiae*. *J Biol Chem* **276**, 10897–10905.

Weber-Lotfi, F., Dietrich, A., Russo, M. & Rubino, L. (2002). Mitochondrial targeting and membrane anchoring of a viral replicase in plant and yeast cells. *J Virol* **76**, 10485–10496.

White, K. A. & Nagy, P. D. (2004). Advances in the molecular biology of tombusviruses: gene expression, genome replication, and recombination. *Prog Nucleic Acid Res Mol Biol* **78**, 187–226.

Zhang, S. C., Zhang, G., Yang, L., Chisholm, J. & Sanfaçon, H. (2005). Evidence that insertion of tomato ringspot nepovirus NTB-VPg protein in endoplasmic reticulum membranes is directed by two domains: a C-terminal transmembrane helix and an N-terminal amphipathic helix. *J Virol* **79**, 11752–11765.